Probing antiferromagnetic coupling between nanomagnets

R. P. Cowburn
Department of Physics, University of Durham, Rochester Building, Science Laboratories, South Road, Durham DH1 3LE, United Kingdom
(Received 20 July 2001; published 13 February 2002)

We have performed an experimental study into magnetostatic coupling between Permalloy nanomagnets arranged in linear chains. By engineering the anisotropy of each nanomagnet, the nanomagnets can be forced to couple in an antiferromagnetic arrangement. Using an experimental method, we show that the antiferromagnetic coupling is perfect for the first four nanomagnets in the chain, but thereafter phase defects arise. Differences between the information transmission capability of ferromagnetic coupling and antiferromagnetic coupling are discussed.

DOI: 10.1103/PhysRevB.65.092409 PACS number(s): 75.75.+a, 78.20.Ls, 81.07.−b

The study of nanometer-sized magnetic particles made by modern nanoscience techniques is a rich and rapidly advancing area within condensed matter physics. Interest in this area comes partly from data storage technology (e.g., hard disk drives[1] and magnetic memory chips[2]) and partly because nanomagnets provide a highly controlled experimental system for studying fundamental phenomena in micromagnetism,[3] transport,[4,5] and statistical physics.[6] Particularly interesting physics occurs when nanomagnets are grouped closely enough to allow strong interactions. These interactions, which are usually either magnetostatic or RKKY in origin, lead to collective behavior, which can dominate over the individual particle properties. Because of the large number of degrees of freedom, interacting ensembles can produce very rich and interesting behavior, such as magnetically driven self-assembly[7] or long-range solitons.[8]

Most studies of magnetostatic interactions have been limited to the *ferromagnetic* coupling between particles: i.e., the average magnetization vector of a given nanomagnet is parallel in direction to that of its neighbor.[9,10] In this paper, we present an experimental study which succeeds in probing the *antiferromagnetic* magnetostatic coupling between nanomagnets arranged in a linear chain. We show that, despite there being no net moment on the system, we are nevertheless able to make local measurements of the antiferromagnetic order parameter and show how it decays as phase defects arise in the chain.

We consider in Fig. 1 a number of thin, circular nanomagnets arranged in a linear chain. If the lateral size of the nanomagnets is sufficiently small (~100 nm or less), then each nanomagnet will be in the single-domain state and can, to first order, be treated as a point dipole which is confined to lie in the plane.[3] Suppose, in addition, that each nanomagnet has a uniaxial anisotropy, the easy axis of which lies transverse to the chain, and that an applied magnetic field also lies in this direction. We consider the three simplest configurations for the chain of moments, which we call ferromagnetic longitudinal (FL), ferromagnetic transverse (FT), and antiferromagnetic transverse (AFT). These configurations are defined in Fig. 1. In determining which configuration will be the system ground state, there are three energy terms to consider: uniaxial anisotropy, dipolar coupling interactions, and Zeeman energy from the applied field. It is simple to show that the energy U of each configurations is

$$\begin{aligned} \text{FL:} \quad & U = -2J, \\ \text{FT:} \quad & U = J - MH - K_u, \\ \text{AFT:} \quad & U = -J - K_u, \end{aligned} \tag{1}$$

where J is the dipolar coupling energy between two antiparallel planar nanomagnets, M is the moment on each nanomagnet, H is the applied field strength, and K_u is the uniaxial anisotropy strength. A simple schematic phase diagram can thus be constructed from Eq. (1), showing the ground-state configuration as a function of J and H. This is shown in Fig. 1. The most interesting scenario is when the coupling is weaker than the uniaxial anisotropy and the applied field is

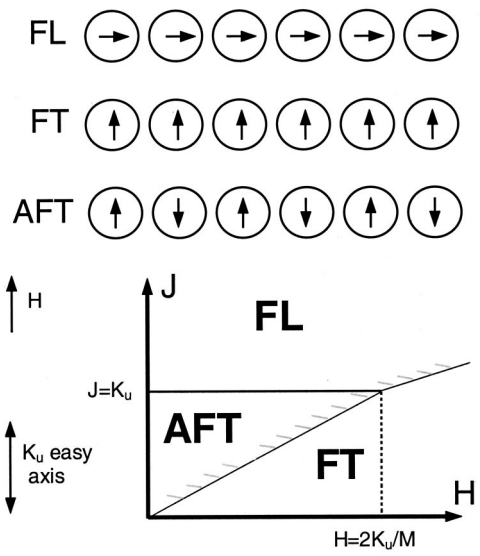

FIG. 1. Definitions of the ferromagnetic longitudinal (FL), ferromagnetic transverse (FT), and antiferromagnetic transverse (AFT) configurations in a planar chain of coupled moments M and a schematic phase diagram giving the expected ground state as a function of applied field strength (H) and dipolar coupling strength (J). The hatched phase boundaries indicate gradual transitions involving continuous rotation of the moments.

very weak. In this case, energy is minimized by adopting the unusual AFT configuration. Unfortunately, this state is extremely difficult to probe experimentally because it carries no net moment.

We have designed an experimental procedure that allows us to use a high-sensitivity magneto-optical method, based on the longitudinal magnetooptical Kerr effect, to probe the AFT configuration. A full description of the magneto-optical apparatus has been presented elsewhere.[11] In order to probe the AFT configuration in chains of, say, eight nanomagnets, we make eight different samples. In the first, only a single nanomagnet is present in each chain. In the second, two nanomagnets are present in each chain, and so on, until the entire chain is complete. We then demagnetize each sample in an oscillating magnetic field of decaying amplitude and look for a magneto-optical signal coming from uncompensated chains with an odd number of nanomagnets and a zero signal coming from fully compensated chains with an even number of nanomagnets. We can thus watch the antiferromagnetic coupling being built up nanomagnet by nanomagnet as the chain length is increased. The apparatus must have sufficient sensitivity to detect the moment of a single nanomagnet. In order to achieve this and in order to check the repeatability of any result, we measure arrays of chains, where the spacing between chains is large enough to avoid interchain dipolar coupling. Further improvements in sensitivity are achieved by dynamically repeating the demagnetizing experiment once every second for several minutes and averaging the Kerr signal.

We engineer the required uniaxial anisotropy by making each nanomagnet slightly elliptical in shape.[12] This generates a small uniaxial shape anisotropy with the easy axis lying along the long axis of the ellipse. It is only possible to probe an array of chains if the phase of the AFT configuration is the same in each chain. We do this by making the first nanomagnet in each chain strongly elliptical and, hence, strongly anisotropic. We then apply a single strong field pulse to the entire sample, which magnetizes the first nanomagnet. Its high anisotropy causes that magnetization state to be retained throughout the rest of the experiment and thus sets the phase of the AFM configuration.

The samples are made using a high-resolution electron beam lithography process with poly(methylmethacrylate) resist, post-development metallization, and liftoff. Full details of the process have been presented elsewhere.[13] The nanomagnets are made from 10-nm-thick Supermalloy ($Ni_{80}Fe_{14}Mo_5$), are 100 nm$\times$120 nm in lateral size, and have a center-to-center spacing of 135 nm within a chain. Figure 2 shows scanning electron micrographs of some of the samples. One can also see in this figure how the chains themselves are formed into a noninteracting array.

Measurement of conventional hysteresis loops shows that the weakly elliptical nanomagnets used throughout the chains have a uniaxial anisotropy field ($=2K_u/M$) of 285 Oe and an interaction field ($=2J/M$) of 75 Oe. The highly anisotropic first nanomagnets had a uniaxial anisotropy field of 580 Oe and a coercive field of 340 Oe. In both cases, the easy-axis loops were very square and the hard-axis loops showed linear slopes with sharp saturation and zero remanence.

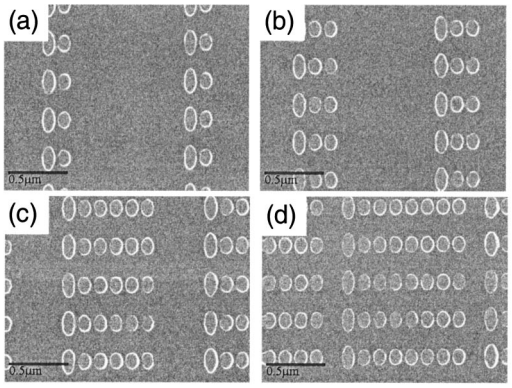

FIG. 2. Scanning electron micrographs of the (a) $n=2$, (b) $n=3$, (c) $n=6$, and (d) $n=8$ samples, where n is the number of nanomagnets per chain.

We now turn to the actual study of the AFT configuration. Figure 3(a) shows, as a function of time, the applied field strength at the *end* of the demagnetization process. $t=0$ is the point at which the next demagnetization cycle begins, and so one sees an abrupt jump in field strength. The maximum field strength during demagnetization is seen to be 290 Oe, which is weaker than the field of 340 Oe required to switch the highly anisotropic first nanomagnet. Figures 3(b)–3(d) show the response to the demagnetization process of samples with, respectively, $n=2$, $n=3$, and $n=4$ (the highly anisotropic first nanomagnet in each chain being magnetized in the *negative* Kerr signal direction). Both the applied field and Kerr sensitivity directions were transverse to the chains. Kerr measurements yield an arbitrary offset to the signal, and

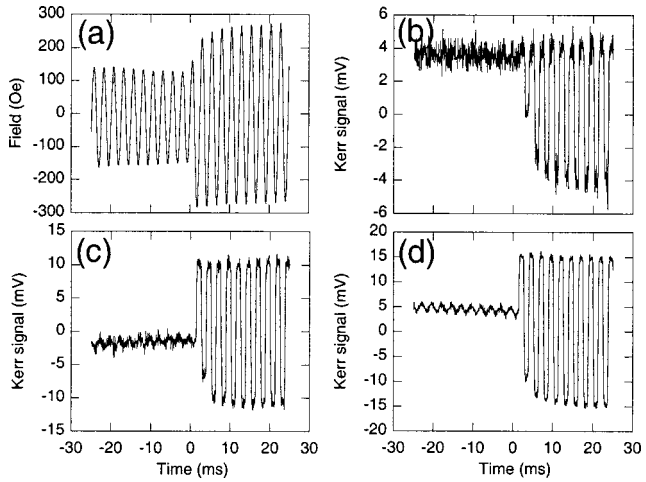

FIG. 3. A time-domain view of the end of the demagnetization process. The decaying envelope finishes at $t=0$, and the field amplitude is abruptly increased, ready to start another decay. (a) shows the oscillating applied magnetic field. The other panels show the Kerr signal for samples (b) $n=2$, (c) $n=3$, and (d) $n=4$, where the highly anisotropic first nanomagnet of each chain had been premagnetized in the negative Kerr direction.

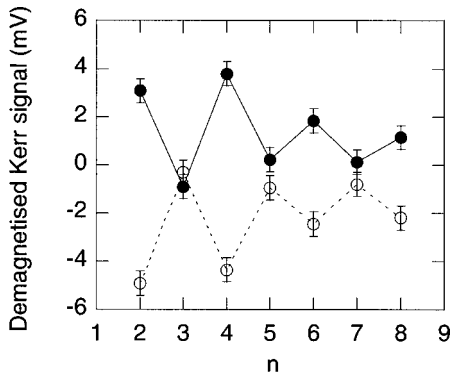

FIG. 4. The Kerr signal at the end of the demagnetizing process for samples with different numbers of nanomagnets per chain, *n*. The highly anisotropic first nanomagnet of each chain was premagnetized in the negative (solid circles) and positive (open circles) Kerr direction.

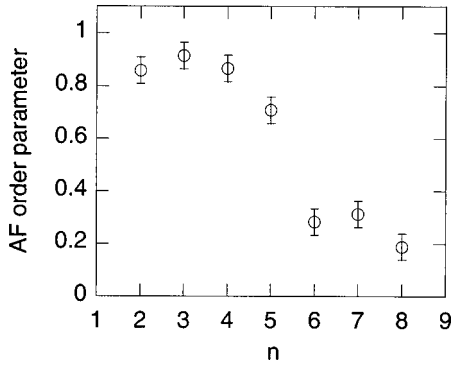

FIG. 5. The experimentally determined antiferromagnetic order parameter measured for different nanomagnet numbers *n* within each chain.

so we use the plus and minus Kerr saturation levels visible in the $t>0$ part of the curves to remove the offset. Note that these saturation levels only refer to the switching of the weakly anisotropic nanomagnets. Consequently, there is no direct contribution to these curves of the highly anisotropic first nanomagnet itself, which makes interpretation of the results much simpler.

One sees that at the end of the demagnetization process, the $n=2$ chains have a net transverse magnetization almost equal to the positive saturation level. This shows that in virtually all of the chains, the second nanomagnet is magnetized in the positive Kerr signal direction, i.e., antiparallel to the highly anisotropic first nanomagnet. This is conclusive evidence that antiparallel coupling is occurring. When a third nanomagnet is added to make the $n=3$ sample [Fig. 3(c)], the demagnetized signal falls to slightly below the zero level. This shows that it is coupling antiparallel to the second nanomagnet, as would be expected for the AFT configuration. The $n=4$ sample [Fig. 3(d)] has a demagnetized signal level equal again to that of the $n=2$ sample [Fig. 3(b)], showing that the fourth nanomagnet has coupled antiparallel to the third.

When we initially magnetize the highly anisotropic first nanomagnet in the *positive* Kerr signal direction, instead of in the negative direction, the sign of the demagnetized levels is found to be reversed, as would be expected if the phase of the antiferromagnetic coupling is being determined by the first nanomagnet.

Figure 4 shows the results of all of the samples, with *n* ranging from 2 to 8, for the two directions of magnetization of the highly anisotropic first nanomagnet. In this figure, we plot the absolute level of the demagnetised Kerr signal. If the AFT configuration were perfect, then one would expect to see the curve oscillate at constant amplitude as each nanomagnet is added. Within experimental error, this is seen to be so for the first four nanomagnets. Thereafter, the oscillations are still clear, and a sign change is still evident when the initial magnetization direction is reversed, but the magnitude of the oscillations decays strongly. This shows that the AFT configuration is perfect for the first four nanomagnets, but thereafter phase defects arise on a statistical basis.

The data of Fig. 4 can be used to calculate a local antiferromagnetic order parameter as a function of nanomagnet number. We define the order parameter λ_n as

$$\lambda_n=(-1)^n\left[\left(\frac{\Delta V_n^+}{V_n^+}-\frac{\Delta V_n^-}{V_n^-}\right)-\left(\frac{\Delta V_{n-1}^+}{V_{n-1}^+}-\frac{\Delta V_{n-1}^-}{V_{n-1}^-}\right)\right], \tag{2}$$

where *n* is the nanomagnet number being considered, $\Delta V_n^{\pm}$ is the demagnetized Kerr signal of a sample with *n* nanomagnets and with the first nanomagnet positively or negatively magnetized, and $V_n^{\pm}$ is the difference between plus and minus saturation Kerr signals for a particular measurement of $\Delta V_n^{\pm}$, i.e., it simply renormalizes $\Delta V_n^{\pm}$ to the range ± 0.5. The most inner parentheses average results from the two different phases of the AFT configuration. The equation then takes the difference between this value and that obtained with one fewer nanomagnet in the chain, to find the contribution made by nanomagnet *n*. The renormalization of λ_n is such that it should lie in the range 1 to -1 and is the correlation function between the average demagnetized state of nanomagnet number *n* and the state expected for a perfect AFT configuration building out from the premagnetized first dot.

Figure 5 shows the measured local antiferromagnetic order parameter as a function of position in the chain of nanomagnets. As discussed above, the AFT configuration is almost perfect (to within experimental measurement error) for the first four nanomagnets. It then decays to a value of 0.2 by the end of an eight-nanomagnet-long chain.

The fall in antiferromagnetic order parameter as one moves along the chain is due to the failure to remove all phase defects, i.e., frustrations, during the demagnetizing process. Figure 6(a) shows schematically one such frustration. The two nanomagnets on either side of the frustration, *Q* and *R*, experience less net interaction field than do nanomagnets far away from a frustration and so can switch at a lower applied field. Consequently, as the oscillating applied magnetic field decays, there will be a time when only nanomagnets next to a frustration can be switched and no others.

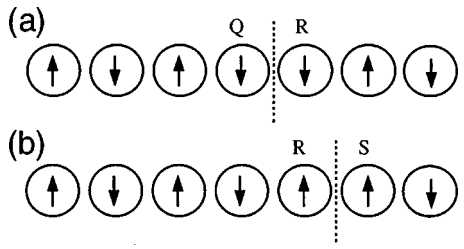

FIG. 6. Schematic representations of a frustration in antiferromagnetic coupling.

This is the time during which the frustrations are mobile. Even though both *Q* and *R* have equally reduced switching fields, it is highly improbable that they will both switch at exactly the same time. Suppose, say, that *R* switches first. Figure 6(b) shows that this causes the frustration to move one step, to lie between *R* and *S*. One of these will then switch on the next half cycle of the oscillating applied field and the frustration will move again. Unfortunately, the direction of motion is not well defined. If the competition to switch depends only on thermal fluctuations, then the frustration would perform a one-dimensional random walk. If other systematic influences are additionally present, such as material defects, then the random walk will be perturbed by traps and barriers. If the frustrations are able to move to the end of the chain or to meet other frustrations, then annihilation occurs and, hence, frustration annealing. However, if systematic material defects exist which can trap the frustration, then complete annealing will not occur. We believe that this is why longer chains are seen not to anneal fully. Other studies in micron-sized systems have found similar incomplete annealing.[14]

It is interesting to think of the antiferromagnetic order parameter as representing the fidelity of the coupled chain of nanomagnets as a communication channel. In a separate experimental study of the FL configuration in chains of isotropic nanomagnets,[8] it was found that 90% reliable communication of the state of a highly anisotropic first nanomagnet could be achieved *even down a chain as long as 69 nanomagnets*. Why is it that the AFT configuration only allows communication through four or five nanomagnets? The difference comes from the way in which the communication vehicle, or frustration, is propagated. In the AFT case, the applied field direction does not encourage a particular propagation direction for the frustration and so the applied field can never force a frustration out of a material defect trap. Conversely, in the FL case, the frustration propagation direction is given by the applied field direction, and so the information vehicle can be forced out of local traps. Frustration annealing is thus much more efficient.

In conclusion, we have investigated antiferromagnetic magnetostatic coupling between planar nanomagnets. We demonstrate that the antiferromagnetic coupling exists largely without defects for the first four nanomagnets of a chain of coupled nanomagnets. Thereafter, frustrations arise which rapidly reduce the order parameter as one moves along the chain. Nevertheless, we have shown that even a chain eight nanomagnets long exhibits some average information transfer from one end to the other, mediated by the antiferromagnetic coupling. These results could find technological application in the biasing of magnetic sensors and memory cells, in ultrahigh-density data storage where interelement interactions must be understood, or in magnetic logic devices.

This work was supported by St John's College, Cambridge and the Royal Society. The author is grateful to Professor M.E. Welland for use of the lithography facilities in the Cambridge University Engineering Department.

[1] S. H. Sun, C. B. Murray, D. Weller, L. Folks, and A. Moser, Science **287**, 1989 (2000).
[2] S. Tehrani, B. Engel, J. M. Slaughter, E. Chen, M. De Herrera, M. Durlam, P. Naji, R. Whig, J. Janesky, and J. Calder, IEEE Trans. Magn. **36**, 2752 (2000).
[3] R. P. Cowburn, D. K. Koltsov, A. O. Adeyeye, M. E. Welland, and D. M. Tricker, Phys. Rev. Lett. **83**, 1042 (1999).
[4] J. A. Katine, F. J. Albert, R. A. Buhrman, E. B. Myers, and D. C. Ralph, Phys. Rev. Lett. **84**, 3149 (2000).
[5] U. Ebels, A. Radulescu, Y. Henry, L. Piraux, and K. Ounadjela, Phys. Rev. Lett. **84**, 983 (2000).
[6] W. T. Coffey, D. S. F. Crothers, J. L. Dormann, Y. P. Kalmykov, E. C. Kennedy, and W. Wernsdorfer, Phys. Rev. Lett. **80**, 5655 (1998).
[7] M. P. Pileni, J. Phys. Chem. B **105**, 3358 (2001).
[8] R. P. Cowburn and M. E. Welland, Science **287**, 1466 (2000).
[9] C. Mathieu, C. Hartmann, M. Bauer, O. Buettner, S. Riedling, B. Roos, S. O. Demokritov, B. Hillebrands, B. Bartenlian, C. Chappert, D. Decanini, F. Rousseaux, E. Cambril, A. Muller, B. Hoffmann, and U. Hartmann, Appl. Phys. Lett. **70**, 2912 (1997).
[10] K. J. Kirk, J. N. Chapman, S. McVitie, P. R. Aitchison, and C. D. W. Wilkinson, J. Appl. Phys. **87**, 5105 (2000).
[11] R. P. Cowburn, D. K. Koltsov, A. O. Adeyeye, and M. E. Welland, Appl. Phys. Lett. **73**, 3947 (1998).
[12] R. P. Cowburn, J. Phys. D **33**, R1 (2000).
[13] R. P. Cowburn, A. O. Adeyeye, and M. E. Welland, Phys. Rev. Lett. **81**, 5414 (1998).
[14] T. Aign, P. Meyer, S. Lemerle, J. P. Jamet, J. Ferre, V. Mathet, C. Chappert, J. Gierak, C. Vieu, F. Rousseaux, H. Launois, and H. Bernas, Phys. Rev. Lett. **81**, 5656 (1998).